Journal of Applied Polymer Science

Silk Fibroin-Chondroitin Sulfate-Alginate Porous Scaffolds: Structural Properties and *In Vitro* Studies

Mitra Naeimi,[1,2] Mohammadhossein Fathi,[1,3] Mohammad Rafienia,[4] Shahin Bonakdar[5]

[1]Biomaterials Research Group, Department of Materials Engineering, Isfahan University of Technology, Isfahan 8415683111, Iran
[2]Isfahan University of Medical Sciences, Isfahan, Iran
[3]Dental Materials Research Center, Isfahan University of Medical Sciences, Isfahan 8174673461, Iran
[4]Biosensor Research Center, Isfahan University of Medical Sciences, Isfahan 81744176, Iran
[5]National Cell Bank of Iran, Pasteur Institute of Iran, Tehran 1316943551, Iran
Correspondence to: M. Naeimi (E-mail: m.naeimi@ma.iut.ac.ir)

ABSTRACT: The development of porous biodegradable scaffolds is of great interest in tissue engineering. In this regard, exploration of novel biocompatible materials is needed. Silk fibroin-chondroitin sulfate-sodium alginate (SF-CHS-SA) porous hybrid scaffolds were successfully prepared via lyophilization method and crosslinked by 1-ethyl-3-(3-dimethylaminopropyl)carbodiimide-ethanol treatment. According to the scanning electron microscopy studies, mean pore diameters of the scaffolds were in the range of 60–187 μm. The porosity percentage of the scaffold with SF-CHS-SA ratio of 70 : 15 : 15 (w/w/w %) was 92.4 ± 3%. Attenuated total reflectance Fourier transform infrared spectroscopy, X-ray diffraction, and differential scanning calorimetry results confirmed the transition from amorphous random coil to crystalline β-sheet in treated SF-CHS-SA scaffold. Compressive modulus was significantly improved in hybrid scaffold with SF-CHS-SA ratio of 70 : 15 : 15 (3.35 ± 0.15 MPa). Cytotoxicity assay showed that the scaffolds have no toxic effects on chondrocytes. Attachment of chondrocytes was much more improved within the SF-CHS-SA hybrid scaffold. Real-time polymerase chain reaction analyses showed a significant increase in gene expression of collagen type II, aggrecan, and SOX9 and decrease in gene expression of collagen type I for SF-CHS-SA compared with SF scaffold. This novel hybrid scaffold can be a good candidate to be utilized as an efficient scaffold for cartilage tissue engineering. © 2014 Wiley Periodicals, Inc. J. Appl. Polym. Sci. **2014**, *131*, 41048.

KEYWORDS: biomaterials; biomedical applications; porous materials

Received 25 March 2014; accepted 19 May 2014
DOI: 10.1002/app.41048

INTRODUCTION

The cocoon of *Bombyx mori* silkworm is mainly composed of sericin and fibroin.[1,2] The silk fibroin (SF) fibers are consisting of two kinds of proteins, a light chain (26 kDa) and a heavy chain (390 kDa), which are linked by a single disulfide bond. These proteins are coated with sericin, a family of hydrophilic proteins (20–310 kDa). The main amino acids present in the SF from *B. mori* are glycine (Gly) (43%), alanine (Ala) (30%), and serine (Ser) (12%).[3] SF is an attractive material for biomedical applications because it has good cell adhesion and growth, low inflammatory response, permeability to oxygen and water, adjustable mechanical properties, slow degradation, and the ease of sterilization. However, scaffolds based on pure SF demonstrate very brittle structure.[1,4–6]

The molecular conformation of SF affects the physical and chemical properties of the final structure. There are two types of molecular conformation for the secondary structure of SF called silk I and silk II. Silk I is a form of SF that is soluble in water and noncrystalline with random coil and α-helix conformations. Conversely, silk II with an organized structure is insoluble in water and highly stable; the β-sheet conformation is called silk II.[2] The rate of degradation of SF scaffold is directly attributed to the amount of β-sheet crystalline structures present within the scaffold. Various processing methods could be used to modify the amount of β-sheet in silk-based biomaterials.[7] To promote the presence of β-sheet conformation in SF scaffolds, some researchers suggested physical and chemical treatments using high temperature, high humidity, and immersion in organic solvents such as methanol.[7] In contrast, the physical properties of SF-based scaffold can be improved by blending it with other natural polymers such as chitosan,[1,4,8,9] elastin,[10] hyaluronic acid,[11] keratin,[12] gelatin,[13] and alginate.[14] Blending SF with other polymers allows the modulation of

Table I. Sample's Compositions and Codes

Sample	SF-CHS-SA scaffold (w/w/w %)	Sample	Treated SF-CHS-SA scaffold (w/w/w %)
100F	100 : 0 : 0	100FT	100 : 0 : 0
90F	90 : 5 : 5	90FT	90 : 5 : 5
70F	70 : 15 : 15	70FT	70 : 15 : 15
50F	50 : 25 : 25	50FT	50 : 25 : 25

biodegradation and release rates, which are important parameters in the biomaterials field.[10]

Sodium alginate (SA) is one of the linear polyanionic copolymers derived from brown algae and composed of 1,4-linked β-D-mannuronic (M) and α-L-guluronic acid (G) residues.[14] Chondroitin sulfate (CHS) is a linear anionic polysaccharide composed of repeated disaccharide units: one of the monosaccharides is *N*-acetyl galactosamine sulfate and the other is glucuronic acid that contains a carboxylate group. CHS has two different chemical structures depending on the position of sulfated group: CHS-C, sulfated on the C6 position of N-acetyl galactosamine and CHS-A, sulfated on the C4 position of *N*-acetyl galactosamine.[15–18] In essence, CHS and SA contain carboxylic groups which are available for carbodiimide-mediated modification. Covalent binding of polysaccharide (CHS and SA) to SF may offers the advantage of extending the degradation time of CHS and SA for better modulation of bioactivity of chondrocytes.[15,19,20]

In this research, porous hybrid scaffolds were prepared from three natural macromolecules: SF, CHS, and SA. Carboxylic groups of CHS and SA were activated by 1-ethyl-3-(3-dimethylaminopropyl)carbodiimide (EDC) solution in order to react with amine groups of SF chains. The effect of the ratio of polysaccharide in the blended scaffold on the porosity and crystallinity of the scaffolds was studied. The structural conformation of the samples was analyzed by attenuated total reflection Fourier transformer infrared spectroscopy (ATR-FTIR) and X-ray diffraction (XRD). The morphology and microstructure of the scaffolds were observed by scanning electron microscopy (SEM). Compressive moduli of the samples were also determined. Thermal properties of the samples were analyzed by differential scanning calorimetry (DSC) technique, 3-(4,5-dimethylthiazol-2-yl)-2,5-diphenyltetrazolium bromide (MTT) assay used to study the *in vitro* cytotoxicity of the scaffolds, and chondrocytes were cultured in the scaffolds to evaluate the cell attachment by SEM analysis and also gene expression was measured by real-time polymerase chain reaction (real-time PCR).

EXPERIMENTAL

Materials

Fresh cocoons of *B. mori* silkworm were purchased from Iranian Silkworm Research Center. CHS, low viscosity SA, and dialysis membrane (molecular-weight cut-off of 12,400 Da) were purchased from Sigma (Sigma-Aldrich, USA). Absolute ethanol, Lithium bromide (LiBr), sodium carbonate (Na_2CO_3), EDC, and *N*-hydroxysuccinimide (NHS) were purchased from Merck chemicals, Germany.

Preparation of Silk Fibroin Aqueous Solution

With slight modification, an aqueous SF solution was prepared according to the method of Rockwood et al.[21] Briefly, silk cocoons were cut into small pieces and degummed with a boiling 0.02*M* Na_2CO_3 solution to remove sericin. After 1 h, they were washed with deionized water and dried at room temperature overnight. Purified fibers were dissolved in 9.3*M* LiBr at 60°C, and then dialyzed against deionized water using a 12 kDa molecular weight cutoff dialysis membrane for 48 h. The final concentration of the prepared aqueous SF solution was determined gravimetrically via drying a determined volume of the solution.[9,21]

Preparation of Scaffolds

The SF aqueous solution (6 w/vol %) was obtained by mentioned process. CHS and SA solutions (6 w/vol %) were prepared by dissolving the CHS and SA powder in distilled water. Different ratios of SF, CHS, and SA solutions were mixed together. The aqueous SF (100 : 0 : 0), SF/CHS/SA (90 : 5 : 5, w/w/w %), SF/CHS/SA (70 : 15 : 15, w/w/w %), and SF/CHS/SA (50 : 25 : 25, w/w/w %) blends were prepared (Table I) and used to fabricate scaffolds. Fabrication of scaffolds was performed by freezing the solution at −20°C, and then lyophilizing (Mini Lyotrap freeze-dryer, LTE, UK) for 48 h at −50°C. The scaffolds were then immersed in the aqueous ethanol solution (70 vol %) containing EDC/NHS (5 m*M* EDC, 2.5 m*M* NHS) at 5°C for 24 h. EDC crosslinking of SF was performed in the presence of ethanol. The crosslinked scaffolds were washed with PBS (pH 7.4) and deionized water. At the final step of process, the crosslinked scaffolds were lyophilized for 24 h at −50°C for next usage.

Porosity Measurements

The porosity of the SF-based scaffolds with different blending ratios was measured by the liquid displacement method. Each sample of prepared scaffolds was immersed in a known volume (V_1) of hexane in a vacuum oven for 30 min. The total volume of hexane after impregnation into the scaffold (V_2) was measured. The scaffold was removed and the residual hexane volume was measured (V_3). The experiment was carried out in triplicate for all different types of the prepared scaffold samples. The porosity percentage of each scaffold (P) was calculated according to the equation[10]:

$$P\ (\%) = \frac{V_1 - V_3}{V_2 - V_3} \times 100 \quad (1)$$

The final determined result for each type of scaffolds was expressed by mean value and standard deviation (SD).

Scanning Electron Microscopy

Freeze-dried scaffolds were sectioned in liquid nitrogen and were sputter-coated with a thin layer of gold. The microstructure of the scaffolds was observed and studied by SEM (Hitachi S4160, Cold Field Emission, Japan). The morphology of the SF scaffold was studied and identified before and after EDC-ethanol treatment. The mean pore diameter of the scaffolds was also calculated by ImageJ (Wayne Rasband, National Institute of

Table II. Primer Sequences for Real-Time PCR

Primer	Sequence	Direction
GAPDH	5′ CGTCTGCCCTATCAACTTTCG 3′	Forward
	5′ CGTTTCTCAGGCTCCCTCT 3′	Reverse
Collagen type I	5′ GCGGTGGTTACGACTTTGGTT 3′	Forward
	5′ AGTGAGGAGGGTCTCAATCTG 3′	Reverse
Collagen type II	5′ CAGGCAGAGGCAGGAAACTAAC 3′	Forward
	5′ CAGAGGTGTTTGACACGGAGTAG 3′	Reverse
Aggrecan	5′ ATGGCTTCCACCAGTGCG 3′	Forward
	5′ CGGATGCCGTAGGTTCTCA 3′	Reverse
SOX9	5′ GTACCCGCACCTGCACAAC 3′	Forward
	5′ TCCGCCTCCTCCACGAAG 3′	Reverse

Health, USA), image analysis software. The diameters of the pores were given as mean value ± SD.

ATR-FTIR Spectroscopy

The ATR-FTIR spectroscopy of the prepared scaffold samples was performed using an ATR-FTIR spectrophotometer (Brucker, Germany). The spectra were recorded between 600 and 4000 cm^{-1}.

X-Ray Diffraction Analysis

An X-ray diffractometer (Siemens, D5000, Germany) with CuK_α radiation was used to phase structural analysis and determine the crystallinity of the scaffolds. Data were collected for 2θ values of 0–35° with a step size of 0.02° and a time per step of 2 sec.

Differential Scanning Calorimetry

Thermal analysis of the samples was performed by DSC apparatus (METTLER TOLEDO, Switzerland) and equipped with N_2 gas flow. DSC measurements were performed from −50°C to 350°C at a heating rate of 10°C min^{-1}.

Mechanical Test

The compressive mechanical analysis was carried out on cylindrical-shaped scaffolds with 6 mm diameter and 8 mm height, according to a modification based on ASTM method F451-95. The tests were performed by a Santam SMT-20 testing machine equipped with a 60 N load cell at room temperature. The crosshead speed was 1 mm min^{-1}, until obtaining a maximum reduction in sample's height of 60%. The compressive modulus of each sample was calculated from the slope of the stress–strain curve at its initial linear section. The values of compressive modulus presented in this report are the average values of three measurements ± SD.

Extraction Method

In order to measure the cell viability percentage, an extraction process was done according to the ISO 10993-5 standard test method. In this procedure, 1 mL of culture medium, Dulbecco's Modified Eagle's Medium (GIBCO, Scotland), was added to each sample with surface area of 3.5 ± 0.5 cm^2. Similar amount of the culture medium was kept in the same condition to be used as a control. The plate was incubated at 37°C with 5% CO_2 for 3 and 7 days. After the specific period of time, the medium of each sample was taken out and used for proliferation test.

Cytotoxicity Assay

Chondrocytes were isolated from rabbit cartilage tissue[22] and cultured into a 96-well microtiter plate at 1×10^4 cells/well. After 24 h, the culture medium of each well was replaced with 90 μL extract of the samples plus 10 μL of fetal bovine serum (Seromed, Germany). After 24 h, the medium of each well were removed and 100 μL of MTT solution (0.5 mg mL^{-1}) was added. The plate was then incubated for 4 h at 37°C in a CO_2 incubator. After this period of time, the purple formazan crystals were dissolved by addition of 100 μL isopropanol for 15 min at 37°C under shaking. The optical density (OD) of each well was recorded at 545 nm using a multiwell microplate reader (STAT FAX-2100) and normalized to the control OD.

Cell Morphology

The chondrocytes were cultured on the surface of the UV-sterilized scaffolds at 2×10^4 cells per 30 μL of culture medium in a 24-well plate. The plate was incubated at 37°C, 5% CO_2. Three hours later, the culture medium (1 mL) was added to each well. After 3 days, the cells were fixed with 4% glutaraldehyde solution. In order to observe and study the chondrocytes morphology by SEM, cellular scaffolds were dehydrated in graded alcohols (10, 30, 50, 70, 80, 90, 95, 100%), each for about 10 min, and sputter-coated with a thin layer of gold. The scaffolds which were seeded with chondrocytes were in circular shape with diameter of 6 mm and thickness of 3 mm.

RNA Extraction and Gene Expression (Real-Time PCR)

The chondrocytes were cultured at a density of 2×10^4 cells within the scaffolds. After 14 days culture, total RNA of the cells was extracted using RNA-isolation kit (Qiagen, RNeasy Plus Mini Kit 50) according to the manufacturer's protocol. The RNA was quantified using spectrophotometer (Nanophotometer, Implen GmbH, Germany) at the wavelength of 260 nm. RNA was converted to cDNA according to the manufacturer's protocol. Each reaction contained 2 μL cDNA sample, 10 μL Real-time Master Mix (Takara), 6 μL water, and 1 μL of each primer. The mixture was incubated at 95°C for 15 min, followed by 40 cycles at 95°C for 15 sec, and 60°C for 1 min. Finally, the mixtures were further evaluated by real-time quantitative PCR instrument (Applied Biosystems, USA). Collagen type I, collagen type II, aggrecan, and SOX9 were chosen as target genes. The primer sequences are listed in Table II. Glyceraldehyde-3-phosphate dehydrogenase (GAPDH) was used as an endogenous housekeeping gene. All experiments were performed in triplicate.

Statistical Analysis

For cell culture studies, statistical calculations were performed using SPSS 16.0 Software with the level of statistical significance set at $P < 0.05$.

RESULTS AND DISCUSSION

SEM Observations

The microstructure of the SF scaffolds before and after EDC-ethanol treatment was studied by SEM (Figure 1). As it is

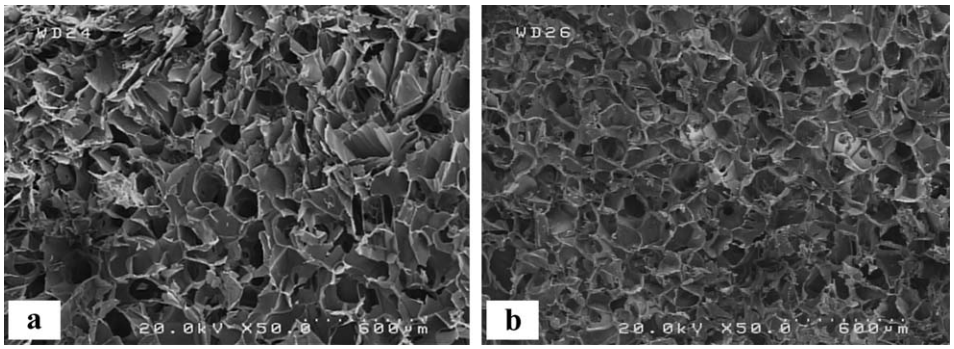

Figure 1. SEM micrographs of the samples, 100F (a) and 100FT (b).

shown in Figure 1(a), the average diameter of the pores was 187.14 ± 3.00 μm, which was calculated by average diameter of 50 pores. A total of 100F scaffold showed a disordered porous structure. Crosslinking the scaffolds by EDC solution and treating by ethanol were used to induce insolubility and conformational transition from random coil to crystalline β-sheet. The microstructure of 100FT scaffold is shown in Figure 1(b). It can be seen that the EDC-ethanol treatment changed the scaffold morphology. A total of 100FT scaffold showed more ordered porous structure. During the crosslinking process, polymer chains could rearrange themselves into a more ordered structure which is beta-sheet conformation. This result is in agreement with the ATR-FTIR and XRD results, which are discussed later. Thus, the structural conformation of SF scaffold was changed under EDC-ethanol treatment. The conformational change was mainly attributed to the swelling of the SF scaffold in ethanol solution. Swelling of the scaffold provided enough space for the rearrangement of molecular chains of SF.

As it is shown in Figure 1(b), the presence of ethanol in this stabilization method preserved the porosity of matrix structure and prevented matrix collapse. Pieper et al. also reported the similar effect of ethanol on preventing matrix structure collapse.[23] Moreover, as could be seen in the SEM image [Figure 1(b)], 100FT scaffold had closed pores in its structure. In the other words, the pores of 100FT scaffold did not have interconnectivity with each other.

Figure 2 shows the influence of CHS and SA ratio on scaffold porous structure. Addition of CHS and SA created more open pores with thinner walls. By introducing CHS and SA into the scaffold, the number of closed pores, which were seen in 100FT scaffold, was decreased and as it can be seen in Figure 2, smaller pores were formed. The internal morphology of 90FT, 70FT, and 50FT scaffolds were significantly influenced by the ratio of the polysaccharide. For example, the mean diameter of the pore of 50FT scaffold was 60.00 ± 5.00 μm, which was less than that of 100FT scaffold (121.45 ± 3.00 μm; Table III).

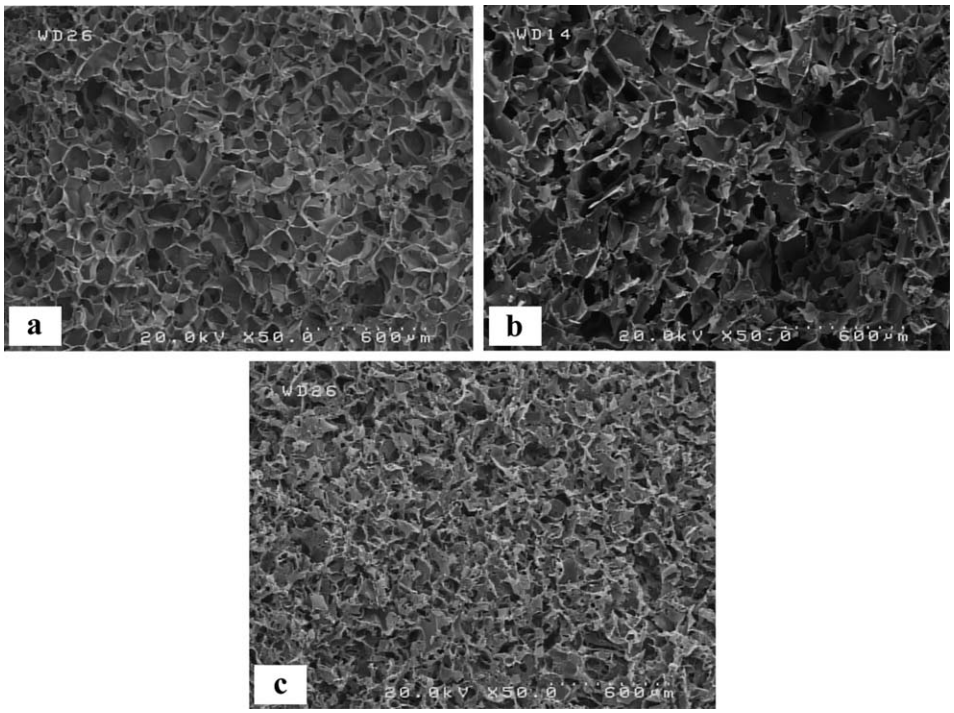

Figure 2. SEM micrographs of the scaffolds after EDC-ethanol treatment, 90FT (a), 70FT (b), and 50FT (c) samples.

Table III. Mean Diameter of Pore of the Scaffolds

Sample code	Mean pore diameter (μm)
100FT	121.45 ± 3.00
90FT	116.80 ± 1.20
70FT	105.50 ± 2.00
50FT	60.00 ± 5.00

The porosity percentage of 100FT and 50FT scaffolds were 78.1 ± 3.5% and 95.3 ± 4%, respectively. Consequently, although the scaffold with higher ratio of the polysaccharide had smaller mean pore diameter, the porosity of the scaffold was higher rather than pure SF scaffold (Figure 3). This fact could be related to the formation of numerous small pores after adding the CHS and SA which could enhance porosity. The results of Yan et al. are in agreement with this aspect.[24]

ATR-FTIR Spectra

The positions of the amide bonds are sensitive to the molecular conformation. Thus, IR spectroscopy is commonly used to investigate the conformation of SF and SF in its blends.[25] The ATR-FTIR spectra of untreated and EDC-ethanol treated scaffolds are shown in Figure 4. A total of 100F scaffold showed peaks at 1648 cm^{-1}, 1530 cm^{-1}, and 1240 cm^{-1} corresponding to amide I, II, and III, respectively. After treatment with EDC-ethanol solution, the amide I and amide II peaks shifted to 1623 cm^{-1} and 1523 cm^{-1} for 100FT scaffold [Figure 4(e)]. Thus, it could be concluded that treatment of the scaffold with EDC-ethanol solution are able to change the conformation of the scaffold. According to the literature, the transition from random coil to β-sheet conformation confirmed by the shifting to lower wavenumbers of amide I (1623 cm^{-1}) and amide II (1523 cm^{-1}) bonds.[26] The ATR-FTIR spectrum of pure CHS [Figure 4(b)] exhibited peaks at 3350 cm^{-1} (OH stretching vibration), 1030 cm^{-1} (C—O—C stretching vibration attributed to the saccharide structure), and 1228 cm^{-1} (S═O

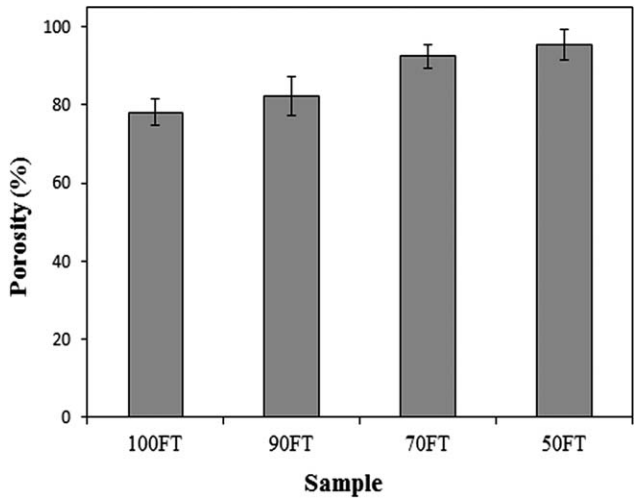

Figure 3. Porosity percentages of the scaffolds after EDC-ethanol treatment.

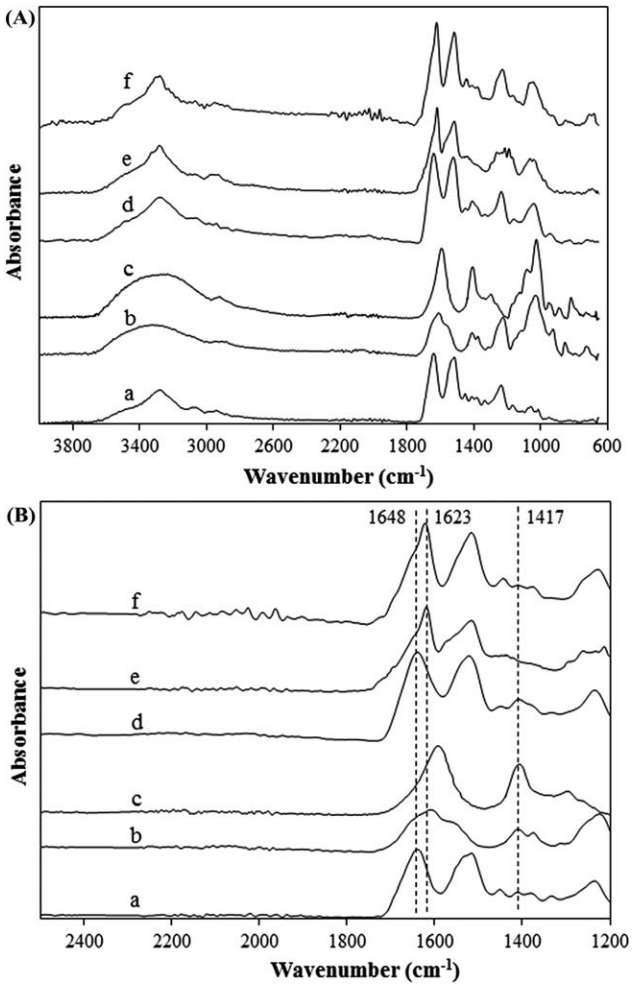

Figure 4. ATR-FTIR spectra of 100F and 100FT sample (a, e), CHS (b), SA (c), 70F, and 70FT sample (d, f), respectively. B: This image is higher magnification of (A).

stretching vibration attributed to the negatively charged SO_4^{2-} groups). In addition, the C—O stretching vibration and O—H variable angle vibration had absorption at 1403 and 1365 cm^{-1}, respectively; they indicated the existence of the free carboxyl groups.[15] The ATR-FTIR spectrum of pure SA was studied [Figure 4(c)]. Generally, the peaks around 3239 cm^{-1}, 1591 cm^{-1}, and 1408 cm^{-1} were attributed to the stretching of O—H, —COO^- (asymmetric), and —COO^- (symmetric), respectively.[14] According to the spectra of 70FT sample, the peak intensity at 1403 cm^{-1} decreased and gradually disappeared with respect to the untreated sample (70F) [Figure 4(d,f)]. It could be related to the interactions occurred between SF, CHS, and SA in the blend after treating with EDC-ethanol solution. Formation of amide bonds between SF, CHS, and SA may involve the consumption of free carboxyl groups in the sample. Thus, it is proved that EDC activated-carboxyl groups of CHS and SA are able to react with the amino groups of SF chains. In the amide III region, 100F and 70F scaffolds had main peak at 1230 cm^{-1} related to random coil conformation [Figure 4(a,d)]. In contrast, 70FT sample had a main peak at 1260 cm^{-1} which is related to beta sheet

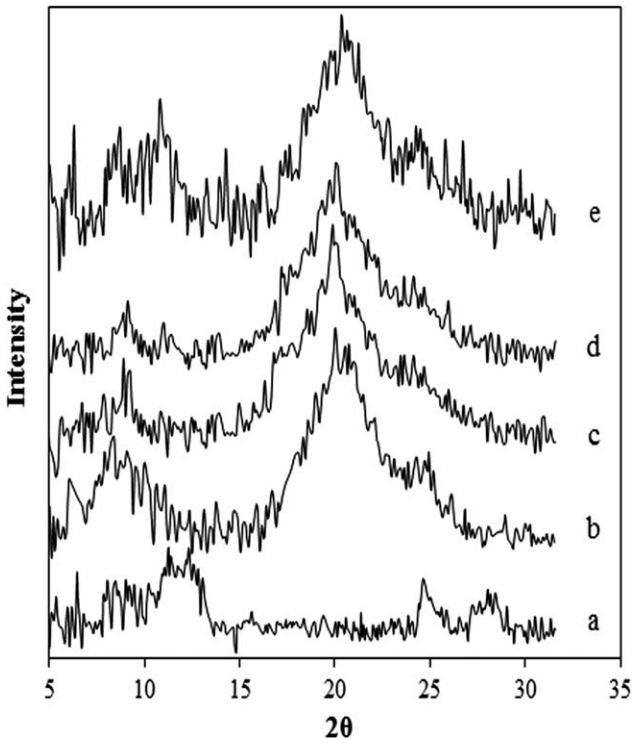

Figure 5. XRD spectra of 100F (a), 100FT (b), 90FT (c), 70FT (d), and 50FT (e) scaffold.

formation [Figure 4(f)]. According to the report of Garcia-Fuentes et al., this shift in wavenumbers may be due to the beta sheet formation.[27]

XRD Phase Structural Analysis

XRD analysis was performed to confirm the conformational changes of the scaffolds. In this case, the diffraction peaks corresponding to silk I and II of SF-based scaffolds were studied. A total of 100FT scaffold could be characterized by the presence of three peaks at 11.45°, 24.68°, and 28.02° corresponding to the silk I crystalline spacing of 7.72, 3.6, and 3.18 Å, respectively [Figure 5(a)]. When the SF scaffold was treated with EDC-ethanol, the diffraction peak at 11.45° which assigned to the silk I structure was disappeared [Figure 5(b)]. However, after treatment, 100FT scaffold exhibited three major peaks at 8.4°, 20.02°, and 24.92° corresponding to the crystalline spacing of 10.5, 4.43, and 3.57 Å related to the growth of the β-sheet structures. Based on the previous studies of researchers, the peak at 20.02° could be assigned to silk II.[28–30] All the peaks were broad and had low intensity, which are indications of low crystallinity of the prepared scaffolds. The results showed that the silk II structure exists in the fibroin sponge after EDC-ethanol treatment. Therefore, XRD results are in agreement and consistent with the ATR-FTIR results to confirm the presence of β-sheet structures in the SF-based scaffold after EDC-ethanol treatment. The XRD patterns of CHS and SA were similar to a typical XRD pattern of an amorphous material consist of a halo without any sharp peaks. A total of 70FT scaffold showed nearly the same pattern as 100FT scaffold [Figure 5(d)]. However, the XRD pattern of 50FT scaffold [Figure 5(e)] showed a little decrease in the intensity of the crystalline peaks.

DSC Spectra

DSC spectra of the samples are shown in Figure 6. The DSC thermograms showed a peak at ~100°C that was attributed to the loss of water during temperature elevation. DSC spectrum of 100F sample showed an endothermic peak at 176°C, which was related to the glass transition temperature (T_g). An exothermic peak at 225°C was ascribed to the crystallization of amorphous SF chains caused by the transition to β-sheet structure. As it was previously observed by the ATR-FTIR and XRD results, the thermal behavior of 100F sample showed a random coil conformation of the SF. An intense endothermic peak at 282°C was related to the decomposition of the SF chains (T_d).[10] DSC spectrum of 100FT scaffold showed that the degradation of the treated scaffolds occurred at two different temperatures, 280°C and 310°C [Figure 6(b)]. One of them may be related to the degradation of amorphous silk I structure (280°C), and the other may be attributed to crystalline silk II structure (310°C). Moreover, the exothermic peak at 225°C disappeared. This is an additional evidence that the SF conformation was changed from random coil to β-sheet after EDC crosslinking. Therefore, EDC-

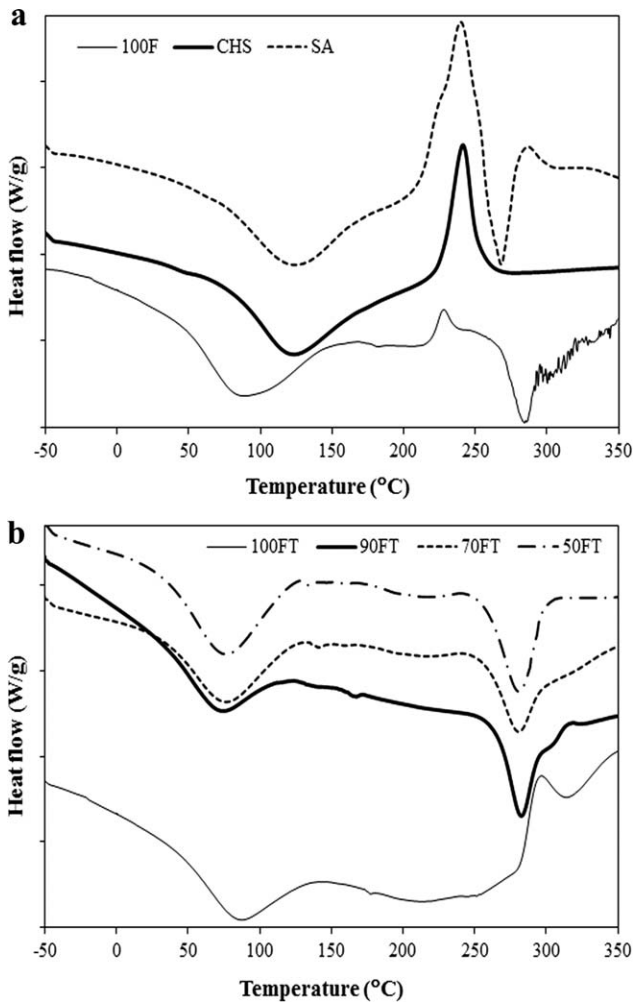

Figure 6. DSC spectra of the scaffolds.

Table IV. Glass Transition Temperature and Thermal Degradation Temperature of the Samples Determined by DSC Spectra

Sample	T_g (°C)	T_d (°C)
100F	176	282
CHS	69	242
SA	101	239
100FT	177	280, 310
90FT	165	282
70FT	141	280
50FT	131	278

ethanol treatment induced an increase in the decomposition temperature. This may be due to the increase in the extent of covalent crosslinks between the chains.[3]

The interaction between SF, CHS, and SA in the sample, which was treated with EDC-ethanol solution, further investigated by using DSC spectrum. The intensive endothermic peaks at 242°C and 239°C [Figure 6(a)] are, respectively, related to decomposition of CHS and SA at high temperature. In 70FT scaffold, CHS and SA degradation peaks (242°C and 239°C) disappeared [Figure 6(b)], it means that there was no phase separation between SF, CHS, and SA. The degradation temperature of 70FT sample was at 280°C. This result indicated that the SF, CHS, and SA not only blended homogenously without phase separation but also formed strong interactions that could change the conformation of SF, CHS, and SA. These events make the conformation and structure of SF, CHS, and SA in 70FT sample different from those of the pure SF, CHS, and SA.[13]

As could be seen in Figure 6(b), the 70FT sample was degraded in a specific decomposition temperature in comparison with 100FT sample which was degraded at two different temperatures. In 70FT scaffold, the degradation completely occurred at 280°C. Thus, the stability of 70FT scaffold was lower than 100FT scaffold. It could be related to the formation of interactions between SF, CHS, and SA. During the interaction of SF, CHS, and SA, their chains may be disordered. Thus, as confirmed by XRD patterns, the interactions may induce a little decrease in the crystallinity of the sample. Mandal and Kundu as well as Polexe and Delair had reported this effect for SF, chitosan, and hyaluronic acid, too.[31,32]

Compatibility of the polymers was also studied by DSC experiment. The DSC curves of CHS and SA [Figure 6(a)] showed endothermic peaks at 69°C and 101°C assigned to the T_g of the polymers, respectively. A total of 70FT scaffold exhibited the T_g at 141°C [Figure 6(b) and Table IV]. DSC spectra showed that the T_g temperatures of the polymers (SF, CHS, and SA) were merged together and 70FT scaffold showed one T_g. Thus, it could be concluded that these polymers are compatible and can be blended homogenously. Moreover, the T_g of 70FT scaffold (141°C) was lower than 100FT scaffold (177°C). Therefore, lower T_g of the scaffold indicated that the crystallinity of the scaffold was decreased.

Mechanical Analysis

The compressive modulus values of the scaffolds are reported in Figure 7. The compressive modulus of 100FT was 2.68 ± 0.20 MPa. The compressive modulus of 70FT was slightly greater among the samples (3.35 ± 0.15 MPa). It can be related to the chemical crosslinking between carboxylic groups of CHS and SA and amino groups of SF. However, compressive modulus of 50FT was decreased significantly (1.02 ± 0.25 MPa). It may be due to the higher porosity and lower crystallinity (XRD results) of 50FT sample. Zhang et al. had reported similar trend for collagen-CHS-hyaluronic acid hydrogel.[33]

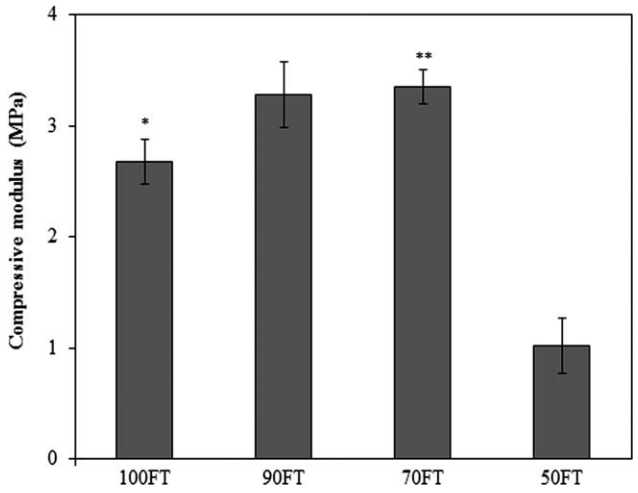

Figure 7. Compressive modulus values of the scaffolds (* and **$P < 0.05$).

Cytotoxicity

The cytotoxic activity of the scaffolds was evaluated using the MTT assay. Figure 8 shows the cell proliferation results for 3 and 7 day's extraction. After exposure with 7 day's scaffold extract, the cell proliferation on 70FT scaffold was enhanced significantly compared to 100FT sample and control group ($P < 0.05$). These results also suggested that 70FT hybrid scaffold with the highest cellular compatibility (among the samples) could promote chondrocyte proliferation.

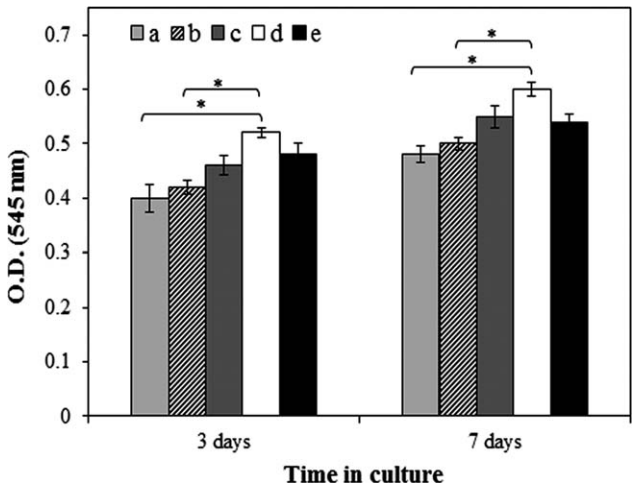

Figure 8. Cell proliferation assessed by MTT test after exposure with 3 and 7 day's scaffold extract: (a) control, (b) 100FT, (c) 90FT, (d) 70FT, and (e) 50FT ($n = 3$; *$P < 0.05$).

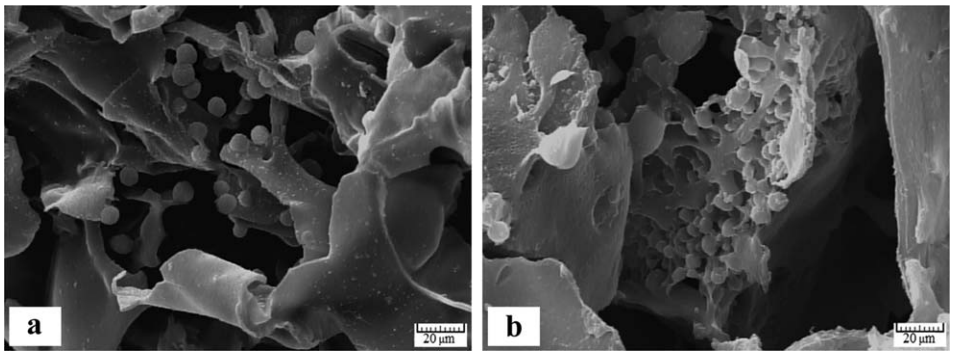

Figure 9. SEM micrographs of the chondrocytes cultured within the scaffolds after 3 days: (a) 100FT and (b) 70FT samples.

Cell Morphology

SEM images of cell growth on the prepared 100FT and 70FT scaffolds are shown in Figure 9. As can be seen in the images, the spherically shaped morphology of the cells is indicative for the chondrocytic phenotype. By observation of the SEM micrographs, it is evident that the initial cell attachment in 70FT scaffold was superior compared with 100FT scaffold and owing to its highly porous structure and interconnected pores. Moreover, glycosaminoglycans are the main components of extracellular matrix of cartilage. Thus, the presence of CHS and SA in the scaffold may promote the adhesion of the seeded chondrocytes.[33,34]

Real-Time PCR

Real time-PCR analysis was carried out to study the gene expression of the cells cultured on the samples. The results of the relative expression levels of the genes in the scaffolds are presented in Figure 10. Chondrocytes grown within 70FT scaffold showed the highest chondrogenic gene expressions of collagen type II, aggrecan, and SOX9 and the lowest gene expression of collagen type I. Aggrecan and collagen type II are in the extracellular matrix of cartilage.[35] In tissue culture polystyrene, as control, and 100FT scaffold the cartilogenous genes were suppressed and the cells were dedifferentiated. Proper differentiation microenvironment is helpful for cell growth, which is in consistent with other reports.[36] Therefore, the differentiation of the chondrocytes could be controlled by the chemical composition, structural conformation (amorphous or crystalline), and compressive modulus of the scaffold. According to the results, SF, CHS, and SA can provide more suitable microenvironment for chondrocytes. The hybrid scaffold could up-regulate chondrogenesis gene expression compared with SF scaffold.

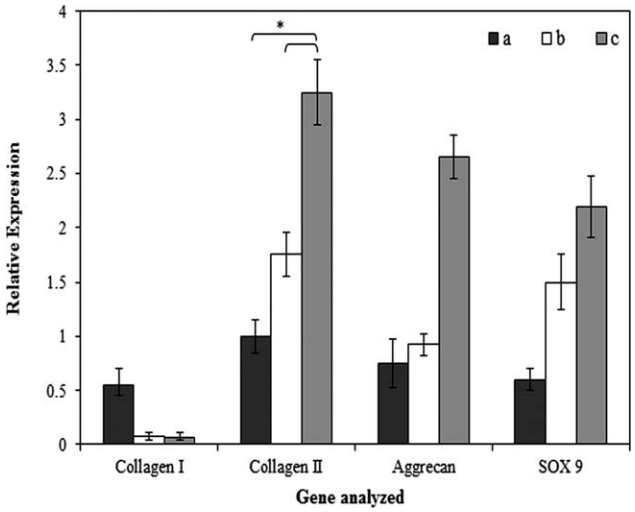

Figure 10. Gene expression of the chondrocytes after 14 days culture within the scaffolds in comparison to tissue culture polystyrene as control group. (a) Tissue culture polystyrene (TCPS), (b) 100FT, and (c) 70FT scaffold ($^*P < 0.01$).

CONCLUSIONS

Novel porous SF-CHS-SA hybrid scaffolds were prepared by freeze-drying of aqueous blended solutions. In order to improve the porosity percentage of the pure SF scaffold, CHS and SA were introduced. Results confirmed that by adding CHS and SA, the mean pore diameter of the scaffolds was decreased while the porosity percentage and interconnectivity of the pores was interestingly increased rather than pure SF scaffold. After EDC-ethanol treatment, chain conformation of the scaffolds changed from amorphous random coil to crystalline β-sheet. Moreover, adding CHS and SA to SF scaffold did not have major effect on the intensity of the crystalline peaks. Compressive modulus was increased significantly in hybrid scaffold compared with untreated SF scaffold. Maximum compressive modulus was related to the scaffold with SF-CHS-SA ratio of 70 : 15 : 15. The attachment and gene expression of the chondrocytes has improved in SF-CHS-SA scaffold rather than untreated SF scaffold. Furthermore, the whole process of preparing scaffolds was all conducted in aqueous media and performed at room temperature, offering possibility to load bioactive drugs or growth factors into the scaffold. According to the good cytocompatibility of the scaffolds combined with other advantages of the scaffolds, these hybrid scaffolds are promising candidates for tissue engineering applications.

REFERENCES

1. Bhardwaj, N.; Kundu, S. C. *Carbohydr. Polym.* **2011**, *85*, 325.
2. Moraes, M. A. d.; Nogueira, G. M.; Weska, R. F.; Beppu, M. M. *Polymers* **2010**, *2*, 719.

3. Vepari, C.; Kaplan, D. L. *Prog. Polym. Sci.* **2007**, *32*, 991.
4. She, Z.; Zhang, B.; Jin, C.; Feng, Q.; Xu, Y. *Polym. Degrad. Stab.* **2008**, *93*, 1316.
5. Bhardwaj, N.; Chakraborty, S.; Kundu, S. C. *Int. J. Biol. Macromol.* **2011**, *49*, 260.
6. Farokhi, M.; Mottaghitalab, F.; Hadjati, J.; Omidvar, R.; Majidi, M.; Amanzadeh, A.; Azami, M.; Tavangar, S. M.; Shokrgozar, M. A.; Ai, J. *J. Appl. Polym. Sci.* **2014**, *131*, 39980.
7. Lawrence, B. D.; Wharram, S.; Kluge, J. A.; Leisk, G. G.; Omenetto, F. G.; Rosenblatt, M. I.; Kaplan, D. L. *Macromol. Biosci.* **2010**, *10*, 393.
8. Sionkowska, A.; Planecka, A. *J. Mol. Liq.* **2013**, *178*, 5.
9. Bhardwaj, N.; Nguyen, Q. T.; Chen, A. C.; Kaplan, D. L.; Sah, R. L.; Kundu, S. C. *Biomaterials* **2011**, *32*, 5773.
10. Vasconcelos, A.; Gomes, A. C.; Cavaco-Paulo, A. *Acta Biomater.* **2012**, *8*, 3049.
11. Yan, S.-Q.; Zhang, Q.; Wang, J.-N.; Li, M.-Z. *J. Fiber Bioeng. Inform.* **2010**, *3*, 62.
12. Vasconcelos, A.; Freddi, G.; Cavaco-Paulo, A. *Biomacromolecules* **2008**, *9*, 1299.
13. Lu, Q.; Zhang, X.; Hu, X.; Kaplan, D. L. *Macromol. Biosci.* **2010**, *10*, 289.
14. Ming, J.; Zuo, B. *Polym. Eng. Sci.* **2013**, *54*, 129.
15. Lai, J.-Y.; Li, Y.-T.; Cho, C.-H.; Yu, T.-C. *Int. J. Nanomed.* **2012**, *7*, 1101.
16. Xiao, X.; He, D.; Liu, F.; Liu, R. *Mater. Chem. Phys.* **2008**, *112*, 838.
17. Ko, C.-S.; Huang, J.-P.; Huang, C.-W.; Chu, I.-M. *J. Biosci. Bioeng.* **2009**, *107*, 177.
18. Peng, C.-K.; Yu, S.-H.; Mi, F.-L.; Shyu, S.-S. *J. Appl. Polym. Sci.* **2006**, *99*, 2091.
19. Richert, L.; Boulmedais, F.; Lavalle, P.; Mutterer, J.; Ferreux, E.; Decher, G.; Schaaf, P.; Voegel, J. C.; Picart, C. *Biomacromolecules* **2004**, *5*, 284.
20. Yang, C. *Bull. Mater. Sci.* **2012**, *35*, 913.
21. Rockwood, D. N.; Preda, R. C.; Yucel, T.; Wang, X.; Lovett, M. L.; Kaplan, D. L. *Nat. Protoc.* **2011**, *6*, 1612.
22. Shokrgozar, M. A.; Bonakdar, S.; Dehghan, M. M.; Emami, S. H.; Montazeri, L.; Azari, S.; Rabbani, M. *J. Mater. Sci.: Mater. Med.* **2013**, *24*, 2449.
23. Pieper, J. S.; Oosterhof, A.; Dijkstra, P. J.; Veerkamp, J. H.; Kuppevelt, T. H. v. *Biomaterials* **1999**, *20*, 847.
24. Yan, S.; Zhang, Q.; Wang, J.; Liu, Y.; Lu, S.; Li, M.; Kaplan, D. L. *Acta Biomater.* **2013**, *9*, 6771.
25. Shang, S.; Zhu, L.; Fan, J. *Carbohydr. Polym.* **2013**, *93*, 561.
26. Lua, Q.; Zhang, B.; Li, M.; Zuo, B.; Kaplan, D. L.; Huang, Y.; Zhu, H. *Biomacromolecules* **2011**, *12*, 1080.
27. Garcia-Fuentes, M.; Giger, E.; Meinel, L.; Merkle, H. P. *Biomaterials* **2008**, *29*, 633.
28. Kim, U. J.; Park, J.; Kim, H. J.; Wada, M.; Kaplan, D. L. *Biomaterials* **2005**, *26*, 2775.
29. Yan, L. P.; Oliveira, J. M.; Oliveira, A. L.; Caridade, S. G.; Mano, J. F.; Reis, R. L. *Acta Biomater.* **2011**, *8*, 289.
30. Kim, U. j.; Park, J.; Li, C.; Valluzzi, R.; Kaplan, D. L. *Biomacromolecules* **2004**, *5*, 786.
31. Mandal, B. B.; Kundu, S. C. *Macromol. Biosci.* **2008**, *8*, 807.
32. Polexe, R. C.; Delair, T. *Molecules* **2013**, *18*, 8563.
33. Zhang, L.; Li, K.; Xiao, W.; Zheng, L.; Xiao, Y.; Fan, H.; Zhang, X. *Carbohydr. Polym.* **2011**, *84*, 118.
34. Venkatesan, J.; Pallela, R.; Bhatnagar, I.; Kim, S. K. *Int. J. Biol. Macromol.* **2012**, *51*, 1033.
35. Wang, C.-C.; Yang, K.-C.; Lin, K.-H.; Liu, Y.-L.; Liu, H.-C.; Lin, F.-H. *Biomaterials* **2012**, *33*, 120.
36. Chen, W.-C.; Yao, C.-L.; Chu, I.-M.; Wei, Y.-H. *J. Biosci. Bioeng.* **2011**, *111*, 226.